Applied Surface Science 254 (2008) 7790–7793

Contents lists available at ScienceDirect

Applied Surface Science

journal homepage: www.elsevier.com/locate/apsusc

Luminescence studies on nitride quaternary alloys double quantum wells

S.C.P. Rodrigues [a,*], O.F.P. dos Santos [a], L.M.R. Scolfaro [b], G.M. Sipahi [c], E.F. da Silva Jr. [d]

[a] Departamento de Física, Universidade Federal Rural de Pernambuco, R. Dom Manoel de Medeiros, s/n - Dois Irmãos, 52171-900 Recife, PE, Brazil
[b] Instituto de Física, Universidade de São Paulo, CP 66318, 05315-970 São Paulo, SP, Brazil
[c] Instituto de Física de São Carlos, Universidade de São Paulo, CP 369, 13560-970 São Carlos, SP, Brazil
[d] Departamento de Física, Universidade Federal de Pernambuco, Cidade Universitária, 50670-901 Recife-PE, Brazil

ARTICLE INFO

Available online 17 February 2008

Keywords:
Photoluminescence
p-Type doping
Nitride semiconductors
Double quantum wells
AlInGaN quaternary alloys

PACS:
73.20 Dx, 78.55.−m, 79.60.Jv, 71.20.N

ABSTRACT

We present theoretical photoluminescence (PL) spectra of undoped and p-doped $Al_xIn_{1-x-y}Ga_yN$/$Al_XIn_{1-X-Y}Ga_YN$ double quantum wells (DQWs). The calculations were performed within the k.p method by means of solving a full eight-band Kane Hamiltonian together with the Poisson equation in a plane wave representation, including exchange–correlation effects within the local density approximation. Strain effects due to the lattice mismatch are also taken into account. We show the calculated PL spectra, analyzing the blue and red-shifts in energy as one varies the spike and the well widths, as well as the acceptor doping concentration. We found a transition between a regime of isolated quantum wells and that of interacting DQWs. Since there are few studies of optical properties of quantum wells based on nitride quaternary alloys, the results reported here will provide guidelines for the interpretation of forthcoming experiments.

1. Introduction

The III-nitride semiconductor materials have undergone an enormous development during the past few years. Of particular interest is the AlInGaN quaternary alloys as potential candidate for developing deep-ultraviolet (UV) light emission diodes and laser diodes [1,2]. It has already been demonstrated the advantages of using AlInGaN quaternary layers, instead of GaN and AlGaN, for the fabrication of high quality quantum structures with strong UV emission at room temperature [3]. Additionally, applications of interest for the quaternary alloys involve long lifetime white lighting, biochemical agent detectors, environment purification, and others [4].

The AlInGaN quaternary alloys have also been studied because they may allow to minimize high densities of threading dislocations, which causes quantum efficiency deterioration. Also, these AlInGaN quaternary allows attaining higher quantum efficiencies as compared to the AlGaN ternary alloys with similar Al contents [4]. Different mechanisms have been proposed for the origin of the luminescence in the AlInGaN quantum well-based devices. It was claimed that the luminescence originates from localized states in In-rich nano-clusters embedded in the wells [5,6]. Other investigations have argued that the optical transitions seen in photoluminescence (PL) spectra originate from quantum wells (QW) states under the influence of strain effects, specially for the wurtzite phase [7,8].

Although there are many reports on the optical investigation of AlGaN/GaN and GaN/InGaN QWs [2], it has been proposed the study of AlGaN/GaN double quantum wells (DQWs) [9] and InGaN/GaN DQWs [10]. However, due to the piezoelectric and spontaneous polarization electric fields existent in the wurtzite phase of the systems, a large internal field is present in the heterostructures. Thus, a quaternary AlInGaN barrier has been used as one way to minimize the internal electric fields [1]. Most of devices are fabricated in the more stable phase, the hexagonal (wurtzite), but there are research efforts towards a more complete understanding of the cubic structures in the last years [11,12]. The absence of polarization fields in the cubic-III-nitrides may be advantageous for some device applications. Moreover the cubic (c) ternary nitride alloys possess potential advantages, as compared to their wurtzite counterparts, such as for the fabrication of laser cavities with cleaved facets [12]. So we assumed the quaternary alloys in the zinc blend (cubic) structure for the calculations. An important feature in the $Al_xGa_yIn_{1-x-y}N$ quaternaries is the possibility to control their energy band gap and lattice constant through the variation of the In and Al compositions in the alloy. We point out that, for the cubic phase, it is possible to reach the red region wavelength with less In content [13]. Another concern of particular interest is the doping in quaternary nitride alloys. Recently, it has been demonstrated that these quaternary alloys may be doped

* Corresponding author. Tel.: +55 81 3320 6487; fax: +55 81 3271 6481.
E-mail address: srodrigues@df.ufrpe.br (S.C.P. Rodrigues).

0169-4332/$ – see front matter © 2008 Elsevier B.V. All rights reserved.
doi:10.1016/j.apsusc.2008.02.034

more easily as p-type, and due to the wavefunction localization the optical transition energies are higher in the alloys than in GaN [14].

In this work we investigate the theoretical photoluminescence spectra in undoped and p-doped $Al_xIn_{1-x-y}Ga_yN/Al_xIn_{1-x-y}Ga_yN$ DQWs, in which the Al and In content, as well as the well and spike widths are varied. Fig. 1 shows a schematic diagram of the DQW systems investigated here. We use a self-consistent Kane method, developed to treat the case of quantum wells and superlattices, in conjunction with the Poisson equation for charge distribution in order to calculate the electronic and optical properties of the systems. Exchange–correlation effects are also included within the local density approximation [15,16]. We assume that all systems are *strained*, so that the optical transitions are due to confinement effects. A detailed discussion of the assumptions made here can be found elsewhere [13]. Our results give important information about the PL spectra in undoped and p-doped AlGaInN-based DQWs, and may be relevant for the interpretation of forthcoming optical measurements.

2. The simulation method

The calculations of the transition energies in the DQWs are carried out by solving the 8×8 Kane multiband effective mass equation (EME). An infinite SL of the square wells forming the DQW, along (0 0 1) direction, is assumed. The multiband EME is represented with respect to plane waves with wavevectors $K = (2\pi/d)l$ (l an integer, d the SL period) equal to reciprocal SL vectors. Rows and columns of the 8×8 Kane Hamiltonian refer to the Bloch-type eigenfunctions $|jm_j\mathbf{k}\rangle$ of Γ_8 heavy and light hole bands, Γ_7 spin-orbit-split hole band and Γ_6 conduction band. $\mathbf{k}$ denotes a vector of the first SL Brillouin zone (BZ). In this representation, the EME assumes the form [13,15,16]

$$\sum_{j'm'K'} (jm_j\mathbf{k}K|T + H_S + V_C + V_{HET} + V_{XC}|j'm'_j\mathbf{k}K') = E(\mathbf{k})(jm_j\mathbf{k}K|E\mathbf{k}) \quad (1)$$

where T is the kinetic energy term, H_s the strain energy originated from the lattice mismatch, V_{HET} the squared potential energy due to the difference between energy gaps, V_{XC} the exchange–correlation potential energy, and V_C is the Coulomb potential energy given by the sum of the Hartree potential V_H and the potential due to the acceptor doping concentration V_A.

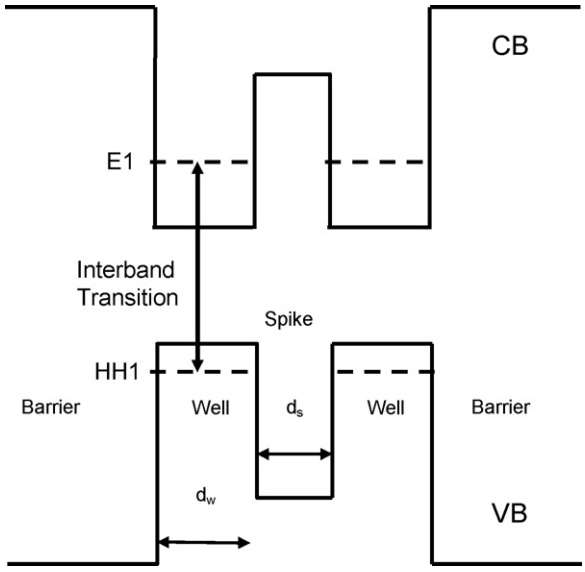

Fig. 1. Schematic diagram for the conduction and valence bands of the DQW structures investigated here. d_w and d_s are the well and the spike widths, respectively. The interband transition is also indicated, as well as the first electron (E1) and heavy hole (HH1) occupied levels.

The self-consistent potentials and charge densities are obtained by solving the multiband EME (1) and the Poisson equation given by

$$(jm_jK|V_C|j'm'_jK') = \frac{-4\pi e^2}{\kappa|K-K'|^2}(K|p(z) - N_A|K')\delta_{jj'}\delta_{m_jm'_j} \quad (2)$$

where κ is the dieletric constant, N_A the acceptor doping concentration and $p(z)$ is the holes charge distribution which is determined by the following equation:

$$p(z) = \sum_{jm_j\mathbf{k} \in \text{empty}} |(zs|jm_j\mathbf{k})|^2 \quad (3)$$

with s being the spin.

From the calculated eigenstates one can determine the luminescence spectra of the systems by applying the following general expression [16]:

$$I(\omega) = \frac{2\hbar\omega^3}{c}\frac{e^2}{m_0c^2}\sum_{\mathbf{k}}\sum_{n_e}\sum_{\substack{n_q \\ q = hh,lh,so}} f_{n_en_q}(\mathbf{k})N_{n_e\mathbf{k}}[1 - N_{n_q\mathbf{k}}] \times \frac{1}{\pi}\frac{\gamma_{n_e\mathbf{k}n_q\mathbf{k}}}{[E_{n_e}(\mathbf{k}) - E_{n_q}(\mathbf{k}) - \hbar\omega]^2 + \gamma^2_{n_e\mathbf{k}n_q\mathbf{k}}} \quad (4)$$

where e is the electron charge, m_0 its mass, ω the incident radiation frequency, γ the emission broadening, n_e and n_q are the electron and hole states associated to the transition, and E_{n_e} and E_{n_q} are the energies associated to them. $N_{n_e\mathbf{k}}$ and $[1 - N_{n_q\mathbf{k}}]$ are the Fermi-like occupation functions for the states in conduction- and valence-band, respectively. The oscillator strength, $f_{n_en_q}(\mathbf{k})$, is given by

$$f_{n_en_q}(\mathbf{k}) = \frac{2}{m_0}\sum_{\sigma_e\sigma_q}\frac{|\langle n_e\sigma_e\mathbf{k}|p_x|n_q\sigma_q\mathbf{k}\rangle|^2}{E_{n_e}(\mathbf{k}) - E_{n_q}(\mathbf{k})} \quad (5)$$

where p_x is the dipole momentum in the x direction, and σ_e and σ_q denote the spin values for electrons and holes, respectively.

The parameters used in the calculations are the same used previously by us [13,15,16]. We consider the gap energy dependence on the Al and In contents for the AlInGaN alloys as described in Ref. [17]. All the other quantities for the alloys were assumed interpolated linearly [13]. The acceptor concentration corresponds to fully p-doped barriers ($Al_{0.25}Ga_{0.70}In_{0.05}N$).

3. Results and discussion

In Fig. 2 we show the theoretical PL spectra at $T = 2$ K for an undoped cubic DQW system constituted of a fixed 10-nm thick well of $Al_{0.25}Ga_{0.70}In_{0.05}N$, a variable width ($d_w$) well of $Al_{0.08}Ga_{0.55}In_{0.37}N$, a variable width ($d_s$) spike well of $Al_{0.10}Ga_{0.80}In_{0.10}N$, again a variable width (d_w) well of $Al_{0.08}Ga_{0.55}In_{0.37}N$ and a fixed 10 nm thick well of $Al_{0.25}Ga_{0.70}In_{0.05}N$. The electronic transitions refer always to the first electron level and the first heavy hole level. We considered spike widths d_s of 8 nm, 6 nm, 5 nm, 4 nm, 3 nm, and 2 nm, as presented in Fig. 2a. In all cases shown in Fig. 2a the $Al_{0.08}Ga_{0.55}In_{0.37}N$ layer width d_w is fixed in 4 nm. It is clearly seen a red-shift in energy as the spike width increases. This effect occurs due to the confinement effects. However, a different behaviour is observed for the optical transitions in the case shown in Fig. 2b, for which we fixed the spike width in 4 nm and the well width d_w was varied, assuming the values 8 nm, 6 nm, 5 nm, 4 nm, 3 nm, and 2 nm. The blue-shifts in energy are found to occur until $d_w = 4$ nm, whereas for $d_w > 4$ nm we observe a red-shift followed by a blue-shift for $d_w > 5$ nm. Therefore, when the thickness of the